Kondo Effect in a Quantum Antidot

M. Kataoka, C. J. B. Ford, M. Y. Simmons,* and D. A. Ritchie
Cavendish Laboratory, Madingley Road, Cambridge CB3 0HE, United Kingdom
(Received 21 May 2002; published 7 November 2002)

We report Kondo-like behavior in a quantum antidot (a submicron depleted region in a two-dimensional electron gas) in the quantum-Hall regime. When both spins of the lowest Landau level are present all around the antidot, the resonances between extended edge states via antidot bound states show an abnormal feature in alternate Coulomb-blockaded regions. The feature becomes suppressed when the temperature or source-drain bias is raised as for Kondo resonances in quantum dots. Although the exact mechanism is unknown, Kondo-like correlated tunneling may arise from a Skyrmion-type edge reconstruction. This observation demonstrates the generality of the Kondo phenomenon.

DOI: 10.1103/PhysRevLett.89.226803 PACS numbers: 73.23.Hk, 72.15.Qm, 73.43.–f

One of the most well-studied many-body phenomena, the Kondo effect, arises in systems where an isolated electronic spin is present in a sea of free electrons, as in metals containing magnetic impurities [1,2]. Recently, the Kondo effect has attracted much attention, since it has been observed in weakly confined quantum dots [3–9], where the discrete levels resemble those in impurities. The flexibility in tuning various parameters has recently enabled the study of Kondo phenomena in great detail. Here we report Kondo-like behavior in a very different system, a quantum antidot [10–13], where electrons are confined magnetically (by the Lorentz force) around a submicron depleted region (antidot) in a two-dimensional electron gas (2DEG). Certain features of our results, such as the absence of spin splitting of the zero-bias anomaly, imply that the system cannot be described by the conventional Kondo models. We suggest that a Skyrmion-type edge reconstruction leads to an enhancement of correlated tunneling between extended edge states via the antidot.

An impurity in a metal (or a quantum dot coupled to reservoirs) is magnetic if it contains an unpaired electronic spin. At low temperature, the second- and higher-order impurity-scattering processes involving spin flip of the localized electron [Fig. 1(a)] are enhanced if the coupling between the localized and delocalized electrons is antiferromagnetic. This is the Kondo effect. As a result, in the metal, the resistivity increases as it is cooled down, the opposite of ordinary metallic behavior. In a quantum dot, the transmission between reservoirs becomes enhanced. Such a Kondo resonance occurs when the dot has an unpaired spin (i.e., when the number of electrons N in the quantum dot is odd). As N is changed by, for example, varying the voltage on a gate nearby, the conductance through the dot shows pairing of resonances at low temperature, as the Kondo effect increases the conductance of alternate Coulomb-blockaded regions, bringing the two peaks close together [the top-right diagram in Fig. 1(a)]. This is often called odd-even behavior.

Now, in terms of device structure, a quantum antidot [Fig. 1(b)] is quite different from a quantum dot. A magnetic field B applied perpendicular to the plane of the 2DEG quantizes the kinetic energy of the electrons into Landau levels (LLs). Along the bulk 2DEG boundaries, the LLs rise in energy with the electrostatic potential, and extended edge states form where the LLs intersect the Fermi energy E_F. Around the antidot, electrons form localized states, traveling phase coherently in closed orbits. Because of the Aharonov-Bohm (AB) effect, each state encompasses an integer number of magnetic flux quanta $\phi_0 = h/e$. Therefore, the average area S_i enclosed by the ith state is quantized as $BS_i = i\phi_0$. The states are filled up to E_F [filled circles in Fig. 1(b)], and those above are empty (open circles). When B increases, each state shrinks in area (in order to keep BS_i constant), moving towards the center of the antidot, and accumulating a net negative charge. Because the states are all

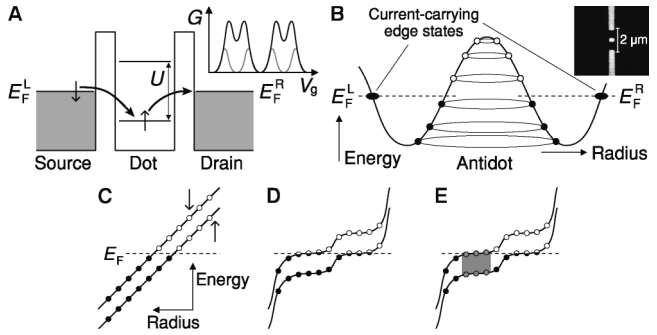

FIG. 1. (a) Spin-flip tunneling through a Coulomb-blockaded quantum dot (U: charging energy). The Kondo effect enhances higher-order processes of such tunneling at low temperature. The top-right diagram shows the conductance G of the dot versus gate voltage V_g with (black) and without (grey) Kondo resonances. (b) A Landau level near the antidot and constrictions. Filled and open circles represent the circular orbits of filled and empty states, respectively. Top-right inset: a scanning electron micrograph of a device prior to the second-layer metallization. (c) A Landau level near the Fermi energy around the antidot with an accidental spin degeneracy between neighboring states. (d) Self-consistent potential with two compressible regions (one for each spin). (e) As (d) but with correlated states (shaded) in the $1 < \nu < 2$ region.

quantized, the net charge cannot relax until enough charge ($-e/2$) has built up, at which point an electron leaves and the net charge jumps to $e/2$ [12]; the process then repeats with period $\Delta B = h/eS$, where S is the area enclosed by a state at E_F. This periodic depopulation can be observed in conductance measurements if the current-carrying extended edge states are brought close to the antidot so that electrons tunnel between them [see Fig. 1(b)]. Here the conductance decreases on resonance, because the resonance enhances backscattering (between opposite edges). This resonance process when sweeping B resembles that when sweeping gate voltage in quantum dots: off resonance, tunneling is Coulomb blockaded due to the discreteness of the electronic charge.

Samples were fabricated from a GaAs/AlGaAs quantum-well structure containing a 2DEG situated 300 nm below the surface with a sheet density 3×10^{15} m^{-2} and mobility 500 m^2/V s. Metal Schottky gates (10 nm NiCr/30 nm Au) were patterned on the surface by electron-beam lithography [top-right inset of Fig. 1(b)]. A second metal layer (30 nm NiCr/70 nm Au) was patterned on top of 350 nm cross-linked polymethyl methacrylate [14] in order to contact the central dot gate so that voltages can be applied to the three gates independently. A negative voltage on the dot gate, 0.3 μm on a side, creates an antidot by depleting electrons underneath. The depleted region can be approximated to be circular, with a radius of ~0.36–0.40 μm, depending on the voltage used; the radius is deduced from the AB period ΔB. The two side gates, which are used to bring the extended edge states close to the antidot, form parallel one-dimensional constrictions, each with lithographic width 0.7 μm and length 0.3 μm. The measurements were performed in a dilution refrigerator with a base temperature ~25 mK.

The conductance measurements were performed as follows. A 5 μV ac excitation at 77 Hz was applied between the Ohmic contacts 1 and 3 shown in the bottom-left inset to Fig. 2, and the current I was measured using a lock-in amplifier. Simultaneously, the diagonal voltage drop V_{dg} between the contacts 2 and 4 was measured. This gives the antidot conductance $G_{ad} = I/V_{dg}$. In the quantum-Hall regime, this four-terminal measurement gives the "true" [15] two-terminal conductance $G_{ad} = \nu_c e^2/h$, where ν_c is the number of filled LLs in the antidot constrictions [16]. The filling factor ν_c and the coupling between the extended edge states and the antidot states can be tuned by the voltages on the side gates, and they were kept as symmetric as possible throughout.

The number of LLs forming antidot bound states is defined by the number of edge states transmitted through the constrictions. Figure 2 shows a typical G_{ad} vs B curve taken at 25 mK when the two spins of the lowest LL encircle the antidot; ν_c decreases from 2 to 1 as B increases. At low B where G_{ad} is close to the $\nu_c = 2$ quantum-Hall (QH) plateau value $2e^2/h$, a series of pairs

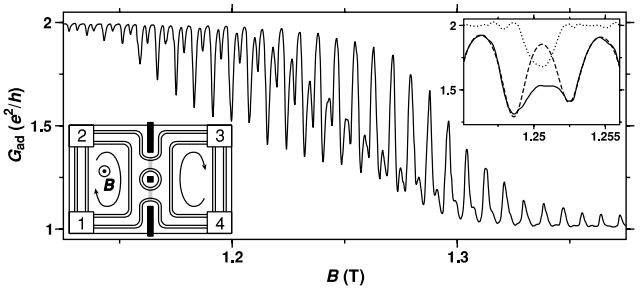

FIG. 2. A typical antidot conductance G_{ad} vs B curve at 25 mK between the $\nu_c = 2$ and 1 plateaux. Top-right inset: the results of a fit conducted for the pair around $B = 1.25$ T by using four dips proportional to the Fermi function derivative. The solid line is the experimental curve and the dashed line is the fit. The fit was performed in such a way that the curves between the pairs match as well as possible (but two dips for the pair can never fit the curve inside the pair). The dotted line is the difference between the experimental curve and the fit (offset by $2e^2/h$). Bottom-left inset: schematic showing the sample geometry with four edge states (solid lines), two of each spin. Arrows indicate the direction of electron flow. Grey lines show where tunneling occurs between the extended edge states and the antidot states. The numbered rectangles on the corners represent Ohmic contacts.

of dips (two dips per ΔB) can be seen. As B increases, and as the coupling between the leads and the antidot becomes stronger (because the edge states move towards the center of the constrictions), the amplitude of the dips increases. Also, the gaps inside pairs (intrapair gaps) seem to be filled up, and eventually the pairs become unrecognizable as two independent dips above 1.3 T as G_{ad} approaches the $\nu_c = 1$ plateau value e^2/h. Very similar G_{ad} curves have been observed between the $\nu_c = 2$ and 1 plateaux with different gate-voltage settings and with different B ranging from 0.8 to 1.5 T in many samples and on many thermal cycles. At higher magnetic fields (> 3 T), the pairing of the resonances disappears, but instead the oscillations become pure double frequency [10,13].

These pairs may simply seem to be spin-split pairs (each dip corresponding to a resonance of either spin). The difference in the amplitude of alternate dips may be an indication of the different coupling strengths for each spin. However, curve fitting (top-right diagram in Fig. 2) shows that the feature in the intrapair gap cannot be explained by such a simplistic model [17]. Strikingly, the paired resonances in Fig. 2, if shown upside down, look very similar to Coulomb-blockade oscillations with Kondo resonances in quantum dots [top-right diagram in Fig. 1(a)]. We argue that the discrepancy in the intrapair gaps is caused by Kondo resonances, based on the results from the nonequilibrium and temperature activation measurements described below.

The behavior of Kondo resonances under nonequilibrium conditions has been well studied in quantum dots [6–9]. Under a finite source-drain bias, mismatch in the

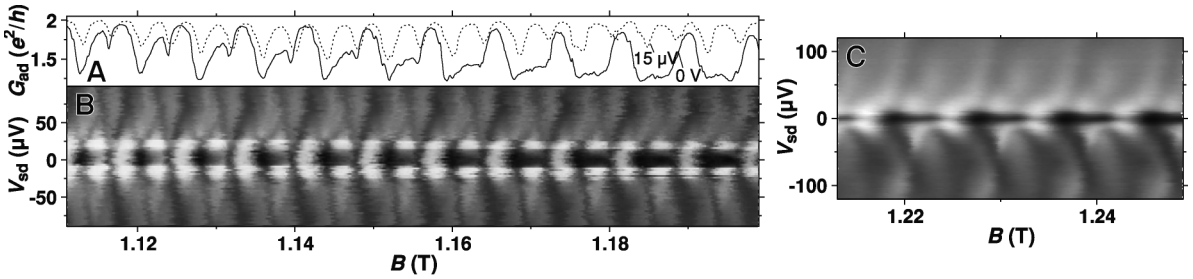

FIG. 3. (a) G_{ad} vs B curves at 25 mK with source-drain bias $V_{sd} = 0$ V (solid line) and with $V_{sd} = 15$ μV (dashed line). The odd-even feature seen at zero bias almost disappears when a small bias is applied. (b) Grey-scale plot of the differential conductance G_{ad} against B and V_{sd} (white: $2e^2/h$, black: $1.2e^2/h$). (c) The dc-bias measurements with stronger coupling plotted in the same manner as in (b) (white: $1.8e^2/h$, black: $1.1e^2/h$).

chemical potentials of the source and drain suppresses the Kondo resonance. In our experiments, when a small source-drain dc bias V_{sd} is applied in addition to the ac excitation, the "Kondo feature" filling each intrapair gap vanishes, leaving two well-defined dips as shown in Fig. 3(a). The Kondo features appear as horizontal dark lines (zero-bias anomaly) along $V_{sd} = 0$ when G_{ad} is plotted in grey scale against V_{sd} and B [Fig. 3(b)]. Note that here the horizontal axis is B instead of V_g, as is normally the case for quantum dots. The zero-bias anomaly becomes stronger as B, and hence the coupling, increases. The diamond-shaped structures of dark lines arise because each resonance splits into two under a finite bias due to the difference in the chemical potentials of the two leads. From the height of each diamond, the energy to add an extra electron (charging energy) can be estimated to be ~ 60 μeV. When the coupling is made even stronger, the zero-bias anomaly is still clearly visible, whereas the diamond structures are smeared out due to weak confinement [Fig. 3(c)].

Increasing temperature T suppresses our Kondo feature, leaving the intrapair gaps better defined [Figs. 4(a) and 4(b)]. At around 190 mK, the intrapair and interpair gaps become almost indistinguishable. At lower B where intrapair gaps are almost as well-defined as interpair gaps, increasing T broadens each dip, and G_{ad} in both gaps decreases (as expected without the Kondo effect). However, at higher B, G_{ad} in the intrapair gaps *increases*. Because the feature disappears into the noise level at relatively low T, it was not possible to study the temperature dependence in more detail, e.g., to determine the Kondo temperature T_K, which normally marks the crossover between logarithmic (high T) and power-law (low T) behaviors. We note that the amplitude of our Kondo feature decreases monotonically as T increases.

The above G_{ad} behavior is qualitatively very similar to that of Kondo resonances in a quantum dot. It appears that as the antidot states are depopulated one by one when B is increased, a localized magnetic moment arises when there is an unpaired electronic spin. Then, when the coupling between the extended and antidot edge states is strong, Kondo resonances enhance the tunneling through the antidot in the Coulomb-blockaded region. Stronger coupling results in larger T_K, and hence the zero-bias anomaly is more pronounced in the region closer to the $\nu_c = 1$ plateau (where the wave functions of the extended and antidot states strongly overlap).

However, there is a crucial difference in our results from those in quantum dots. In a quantum dot in a comparable B, the Zeeman energy $E_Z = |g|\mu_B B$ usually splits the zero-bias anomaly into two parallel lines separated by $2E_Z/e$ (μ_B is the Bohr magneton and $g = -0.44$

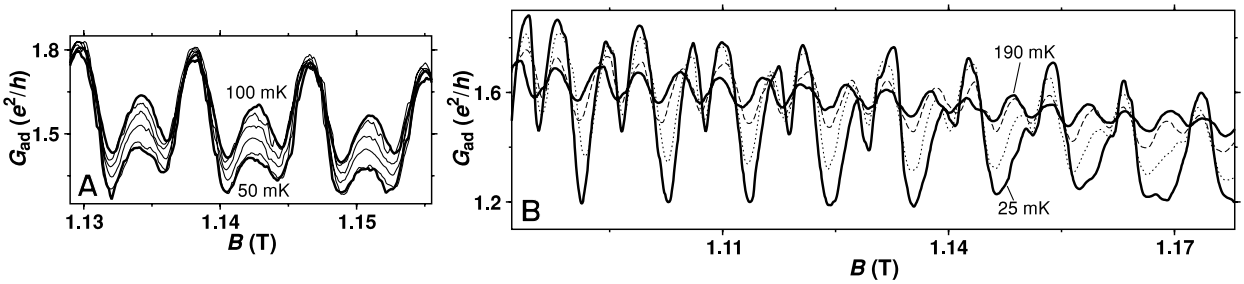

FIG. 4. (a) Temperature dependence of G_{ad} vs B with small increments of temperature (~ 10 mK). The feature filling the gap inside each pair weakens as the temperature T is increased, leaving the gaps inside pairs *better* defined at *higher* temperature, which is a signature of the Kondo effect. (b) Temperature dependence of G_{ad} vs B over a wide range of T. The odd-even feature at low T disappears as T is raised to 190 mK, showing almost double-frequency oscillations.

in bulk GaAs). The Kondo resonance is suppressed at $V_{sd} = 0$ because spin degeneracy is lifted [6,7,9]. At $B = 1.2$ T, $E_Z = 30$ μeV, but the width of our zero-bias anomaly is ~ 20 μV. Thus, the energy gap between the opposite spin states must be at most 10 μeV, and probably much smaller. This is at least a factor of 3 less than E_Z.

One possible explanation for this lack of spin splitting is an accidental degeneracy between neighboring orbital states with opposite spins. This might occur if E_Z happened to be close to an integer multiple of the single-particle energy spacing ΔE_{sp} [the difference in potential energy between neighboring states; see Fig. 1(c)]. However, since $\Delta E_{sp} \propto 1/B$ if a constant potential is assumed, the ratio $E_Z/\Delta E_{sp} \propto B^2$ would not stay constant over a wide range of B. As we have observed the effect under various conditions, it is highly unlikely that this accidental degeneracy is the cause.

Another important issue in our experiments is that dips in G_{ad} saturate at e^2/h (Fig. 2), forming the $\nu_c = 1$ plateau as B increases and the oscillations die away. The existence of the $\nu_c = 1$ plateau implies that the extended edge states of the lower spin are perfectly transmitted through the constrictions, and not coupled to the antidot. This causes another difficulty in the interpretation, because, for Kondo resonances to occur, both spins in the leads need to be coupled to the localized state.

It is likely that the edge-state picture shown so far needs to be modified to a many-body picture. Recently, we have demonstrated that a self-consistent treatment of the antidot potential is important, especially at higher B [13]. Taking into account the formation of two concentric compressible rings, where states are partially filled, and are pinned at E_F [Fig. 1(d)] [18], we have successfully explained double-frequency AB oscillations observed at higher B [10]. However, this is not yet enough for the Kondo effect, as either only one spin (outer ring) would be coupled to the leads, or, if both spins were coupled to the leads, there would be no $\nu_c = 1$ plateau.

It has been shown that in a relatively weak magnetic field, an excited state of a $\nu = 1$ QH liquid is not simply a spin flip, but rather, a complicated spin texture, called a Skyrmion [19], which forms due to strong correlations. Recent work has shown that Skyrmion-type edge reconstruction is important in quantum dots in the QH regime [20,21]. If we assume that such correlated states form in the regions of the antidot and extended edge states where the local filling factor is $1 < \nu < 2$ [Fig. 1(e)], electrons with both spins there would be allowed to tunnel, whether the $\nu \leq 1$ edge states are coupled or not. The excitation energy of correlated states is typically smaller than E_Z. If two configurations, in which the total spin differs by one, are (almost) degenerate, this may allow spin-flip tunneling. It is uncertain, however, whether the odd-even behavior can occur with such strongly correlated states. It may be appropriate to treat the antidot as a dot of holes.

In summary, we have shown that an antidot in the quantum-Hall regime qualitatively exhibits all the features of the Kondo effect, despite the lack of an obvious reason for spin degeneracy. We have suggested possible ways in which the edge-state picture may be modified to take account of interactions. The fact that the antidot is an open system further complicates the problem, in comparison with quantum dots, where only a limited number of states are considered. A detailed theoretical calculation is needed to determine the edge-state structure that gives rise to the Kondo-like behavior in an antidot.

This work was funded by the U.K. EPSRC. We thank I. Smolyarenko, N. R. Cooper, B. D. Simons, C. H. W. Barnes, A. S. Sachrajda, H.-S. Sim, and V. Falko for useful discussions.

*Present address: School of Physics, University of New South Wales, Sydney 2052, Australia.

[1] J. Kondo, Prog. Theor. Phys. **32**, 37 (1964).
[2] For a review, see A. C. Hewson, *The Kondo Problem to Heavy Fermions* (Cambridge University Press, Cambridge, 1993).
[3] L. I. Glazman and M. E. Raikh, JETP Lett. **47**, 452 (1988).
[4] T. K. Ng and P. A. Lee, Phys. Rev. Lett. **61**, 1768 (1988).
[5] Y. Meir, N. S. Wingreen, and P. A. Lee, Phys. Rev. Lett. **70**, 2601 (1993).
[6] D. Goldhaber-Gordon *et al.*, Nature (London) **391**, 156 (1998).
[7] S. M. Cronenwett, T. H. Oosterkamp, and L. P. Kouwenhoven, Science **281**, 540 (1998).
[8] W. G. van der Wiel *et al.*, Science **289**, 2105 (2000).
[9] M. Keller *et al.*, Phys. Rev. B **64**, 033302 (2001).
[10] C. J. B. Ford *et al.*, Phys. Rev. B **49**, 17 456 (1994).
[11] V. J. Goldman and B. Su, Science **267**, 1010 (1995).
[12] M. Kataoka *et al.*, Phys. Rev. Lett. **83**, 160 (1999).
[13] M. Kataoka *et al.*, Phys. Rev. B **62**, R4817 (2000).
[14] I. Zailer *et al.*, Semicond. Sci. Technol. **11**, 1235 (1996).
[15] "True" in the sense that the two-terminal conductance is not affected by the series resistance of the circuit.
[16] M. Büttiker, Phys. Rev. Lett. **57**, 1761 (1986).
[17] In Ref. [13], we gave a model with transmission and reflection resonances in an attempt to explain similar oscillations; however, this model does not explain the temperature and source-drain bias measurements shown here.
[18] D. B. Chklovskii, B. I. Shklovskii, and L. I. Glazman, Phys. Rev. B **46**, 4026 (1992).
[19] S. L. Sondhi *et al.*, Phys. Rev. B **47**, 16 419 (1993).
[20] P. Hawrylak *et al.*, Phys. Rev. B **59**, 2801 (1999).
[21] C. Tejedor and L. Martin-Moreno, Phys. Rev. B **63**, 035319 (2001).